Error-based Learning Mechanism for Fast Online Adaptation in Robot Motor Control

Mathias Thor and Poramate Manoonpong

Abstract—Existing state-of-the-art frequency adaptation mechanisms of central pattern generators (CPGs) for robot locomotion control typically rely on correlation-based learning. They do not account for the tracking error that may occur between the actual system motion and CPG output, leading to loss of precision, unwanted movement, inefficient energy locomotion, and in the worst cases, motor collapse. To overcome this problem, we developed online error-based learning for frequency adaptation of CPGs. The learning mechanism used for error reduction is a novel modification of the Dual Learner (DL) called Dual Integral Learner (DIL). As well as being able to reduce tracking and steady-state errors, it can also perform fast and stable learning, adapting the CPG frequency to match the performance of robotic systems. Control parameters of the DIL are more straightforward for complex systems (like walking robots), compared to traditional correlation-based learning, since they correspond to error reduction. Due to its embedded memory, the DIL can relearn quickly and recover spontaneously from previously learned parameters. All these features are not covered by existing frequency adaptation mechanisms. We integrated the DIL into a neural CPG-based motor control system for use on different legged robots with various morphologies for evaluation. The results show that: 1) the DIL does not require precise adjustment of its parameters to fit specific robots, and 2) the DIL can automatically and quickly adapt the CPG frequency to the robots such that the entire trajectory of the CPG can be precisely followed with very low tracking and steady-state errors. Consequently, the robots can perform the desired movements with more energy-efficient locomotion compared to the state-of-the-art correlation-based learning mechanism called Frequency Adaptation Through Fast Dynamical Coupling (AFDC). In the future, the proposed error-based learning mechanism for fast online adaptation in robot motor control can be used as a basis for trajectory optimization, universal controllers, and other studies concerning the change of intrinsic or extrinsic parameters.

Index Terms—Central pattern generator, Adaptive oscillator, Locomotion, Energy efficiency, Frequency adaptation, Rhythmic task, Tracking error

I. INTRODUCTION

CENTRAL pattern generators (CPGs) play a crucial role in the control of animal locomotion. A CPG is a group of interconnected neurons that can be activated to generate a motor pattern without the requirement of sensory feedback (for reviews see [1], [2]). As described in [1], various CPG models

M. Thor and P. Manoonpong are with the Embodied AI & Neurorobotics Lab, Centre for BioRobotics, The Mærsk Mc-Kinney Møller Institute, The University of Southern Denmark, Odense M, DK-5230, Denmark. P. Manoonpong is also with the College of Mechanical and Electrical Engineering, Nanjing University of Aeronautics and Astronautics, China and School of Information Science & Technology, Vidyasirimedhi Institute of Science & Technology (VISTEC), Thailand. E-mail: mathias@mmmi.sdu.dk & poma@nuaa.edu.cn.

with different levels of complexity have been proposed; a conceptual biological model called the half-center model [3], detailed biophysical models [4], connectionist models [5], and abstract models [1], [2].

Most biophysical models use Hodgkin-Huxley neurons [4] to investigate the problem of rhythmogenesis, i.e., the generation of rhythmic activity in small neural circuits as well as in the pacemaker properties of single neurons. Connectionist models use simplified neuron models [5], like leaky-integrator neurons or integrate-and-fire neurons, to investigate how a rhythmic activity is generated by network properties, and how different oscillatory neural circuits become synchronized via interneuron connections for limb coordination.

In the domain of robot control, most research has employed abstract models, using coupled oscillators to generate basic periodic patterns of movement. Commonly-used abstract CPG models include the Van der Pol oscillator [6], Matsuoka oscillator [7], and SO(2) or two-neuron oscillator [8]. Most of these CPGs can only generate periodic patterns. Although none of the abstract models require an external input or sensory feedback to produce basic rhythmic activity, they need sensory feedback to adapt their frequency, phase, and amplitude for efficient motor control. For this reason, different adaptation techniques have been developed.

Amplitude adaptation is used for scaling a system's movement, which for a legged robot could facilitate turning and leg lifting behaviors [9]. Turning behaviors often rely on exteroceptive feedback e.g., from foot contact and vision, while leg levitation behaviors often rely on proprioceptive feedback e.g., from joint angles and force. Other approaches include robotic arms that must learn the frequency and amplitude of an external force applied to their effectors [10].

Phase adaptation is often used to generate self-organized locomotion (i.e., joint/leg synchronization). For instance, Owaki et al. [11], Tao et al. [12], and Arena et al. [13] presented approaches to control the legs of a quadruped robot based on decoupled simple CPGs with continuous phase modulation. Instead of predefining the CPG phase relationships, they modulated the CPG phases with respect to the leg load sensing. This resulted in flexibility and adaptability for dealing with changes in weight distribution and locomotion speed.

Frequency adaptation, which is the focus of this study, is most often used to exploit the natural dynamics which may lead to more energy-efficient motion [14]. Typically, the joint angle and foot contact feedback is used to entrain the frequency of a CPG. If the feedback entrains the CPG and it adapts only temporarily (i.e., the feedback has only a short term, transient effect), it is called a reactive CPG [15]. In

this case, if the feedback is switched off, the CPG system immediately returns to its intrinsic dynamics. The reactive CPG, therefore, has no memory of the input and cannot sustain a lasting change to the dynamics. To maintain its effect even when the feedback has been removed, Righetti et al. [16] introduced a frequency adaptation schema which modifies the intrinsic frequency of a CPG permanently. A CPG with this schema is commonly referred to as an adaptive frequency oscillator (AFO). However, a classical AFO with constant feedback strength requires a relatively long adaptation time. To obtain fast and precise adaptations, Nachstedt et al. [17] proposed novel frequency adaptation through fast dynamical coupling (AFDC). This mechanism is based on dynamically adapting the coupling strength of sensory feedback to a CPG.

The above-mentioned frequency adaptation mechanisms all rely on correlation-based learning and work by matching the phase of the CPG to that of a sensory feedback signal. An example is when a correlation-based learning mechanism (like AFO or AFDC) is used to drive a simple system with one degree of freedom, such as a pendulum system using a CPG [18], [19]. The most energy-efficient control is achieved if the pendulum is driven at its resonant frequency given by a phase shift of $\pi/2$ between the applied torque and angular position of the pendulum. By using the angular position as sensory feedback, the correlation-based learning mechanism can be configured to obtain a phase shift of $\pi/2$ between the sensory feedback and the CPG driving the system.

While it is easy to determine the desired phase shift between CPG and sensory feedback signals for a mathematical pendulum and other simple systems, this is not the case for complex systems with many degrees of freedom [20], [21], [22], [23], [24]. In this case, the phase shift has to be determined experimentally since no intuitive relationship exists between the desired phase shift and energy-efficient movement. Furthermore, correlation-based learning does not account for the tracking error that may be present between the CPG output and actual system movement. Such an error could occur from poor motor performance, a lack of power (e.g., the discharge curve of a power source), a wrongly tuned CPG frequency, increased joint load, or varying robot morphologies. The consequences of such an error include loss of precision, unwanted movement, energy-inefficient locomotion, and in the worst case, motor collapse. Furthermore, the tracking error may impact on the performance of the control system in use since the desired trajectory is not as expected. This is especially critical in research concerning trajectory optimization.

To solve this problem, we propose here for the first time, fast online error-based learning for frequency adaptation of a CPG. Using error feedback such as the tracking error between a CPG output and the joint angle sensory signal of a complex robotic system, error-based learning ensures that the CPG frequency matches the performance of the system. By doing so, the entire trajectory, as generated by the CPG, is followed with low tracking error. Another advantage of error-based learning mechanisms, in general, is the fact that they use simple learning parameters that directly relate to error reduction. The learning mechanism used for error reduction in this work is a novel model called the Dual Integral Learner (DIL) which
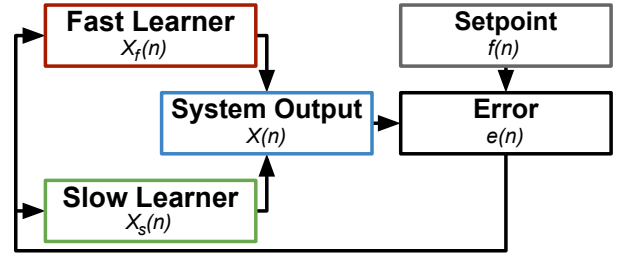

Fig. 1. Block diagram of the DL. The system output, $X(n)$, is the sum of the outputs from the fast and slow learners ($X_f(n)$ and $X_s(n)$ respectively). The error, $e(n)$, is calculated as the difference between the system output and the setpoint, $f(n)$. The error is fed back into the two learners, which both try to reduce it.

is a modification of the Dual Learner (DL) by Smith et al. [25]. The DIL has several advantages when compared to both single-state models (e.g., classical P, PI, PID control) and two-state gain specific models [25], [26]. These include fast and stable learning, savings in relearning, tracking error and steady-state error reduction, and spontaneous recovery of previously learned parameters (see Sect. II-A). Furthermore, the DIL stresses the simplicity of error-based learning. It relies only on a simple objective function (i.e., tracking error feedback) rather than multiple complex objective functions and a system kinematic or dynamic model. Thus, it can be simply applied to other systems providing tracking error feedback which need to reduce error for performance improvement.

The main contributions of this work are thus: (1) to introduce our novel error-based learning mechanism (sect. II-A) and (2) to demonstrate how to implement the error-based learning mechanism with a CPG on different legged robots for quick online frequency adaptation and energy-efficient locomotion with low tracking error (sects. II-A and III). Finally, the mechanism is evaluated using simulated legged robotic systems against the state-of-the-art correlation-based learning mechanism AFDC to determine the strengths of an error-based approach (sects. IV and V).

II. MATERIALS AND METHODS

In this section, we describe the error-based learning mechanism DIL in addition to introducing a neural CPG model and the state-of-the-art correlation-based AFDC [17]. Finally, we describe the experiments conducted to evaluate error-based frequency adaptation (DIL) against correlation-based frequency adaptation (AFDC).

A. Error-based Learning

The DIL is a modified version of the DL presented by Smith et al. [25]. The key idea of the original DL, as explained below, is to use a simple two-state gain specific multi-rate model consisting of two learners acting on different time scales (i.e., fast and slow learners) and in parallel as shown in Fig. 1. Each learner receives the same error and incorporates a proportion of the error into their current estimation of the perturbation [27]. This is shown in the following equations and also presented in [25]:
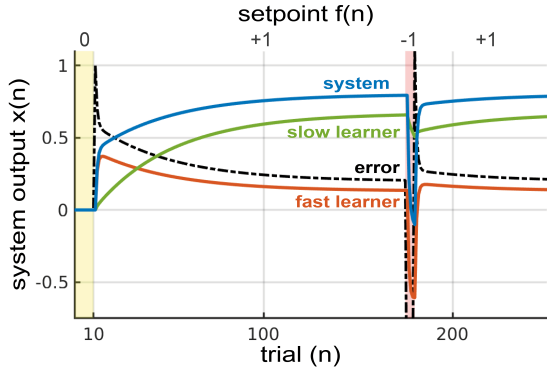
Fig. 2. Simulation of learning in the DL when exposed to a square wave setpoint input. The setpoint is 0 in the yellow zone, +1 in the white zones, and -1 in the red zone. The slow learner's output is shown in green, the fast learner's output in red, and the system output in blue. The error, shown in dashed black, is not fully removed (the system has a steady-state error).
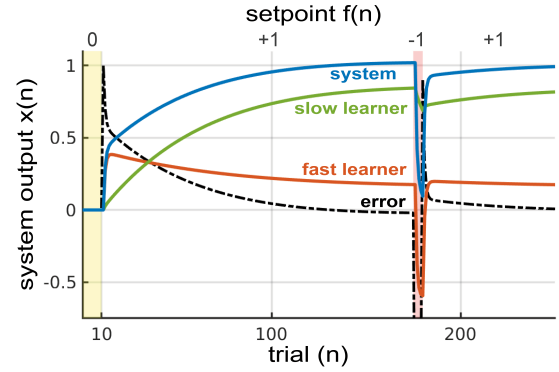

Fig. 3. Simulation of learning in the DIL when exposed to a square wave setpoint input. The setpoint is 0 in the yellow zone, +1 in the white zones, and -1 in the red zone. The slow learner's output is shown in green, the fast learner's output in red, and the system output in blue. The error, shown in dashed black, is reduced to zero.

$$
\begin{aligned}
x_f(n) &= A_f \cdot x_f(n-1) + B_f \cdot e(n) \\
x_s(n) &= A_s \cdot x_s(n-1) + B_s \cdot e(n) \\
x(n) &= x_s(n) + x_f(n) \\
e(n) &= f(n) - x(n)
\end{aligned}
\tag{1}
$$

where $x_f(n)$ is the output of the fast learner, $x_s(n)$ is the output of the slow learner, $x(n)$ is the combination of the two outputs, $e(n)$ is the error given as the difference between the output $x(n)$ and setpoint $f(n)$, B_f and B_s are learning rates, and A_f and A_s are retention factors. The parameter selection is under the constraint that $B_f > B_s$ and $A_f < A_s$. Thus, the fast learner learns more rapidly as indicated by a higher learning rate but also forgets more rapidly as indicated by a lower retention factor.

The main advantages of the interaction between the two learners include fast and stable learning, savings in relearning, tracking error reduction, and spontaneous recovery of previously learned parameters. These advantages are all shown in Fig. 2, demonstrating a simulation of learning in the DL. In the beginning, when the setpoint is instantaneously changed from 0 (yellow zone) to +1 (white zone), the system output (blue line) increases to reduce the error (dashed black line). Firstly, the fast learner (red line) contributes most to the learning process but decays over time resulting in the slow learner (green line) taking over. When the setpoint is set briefly to -1 (red zone), the system output quickly unlearns as the fast learner tries to adapt. It should be noted that in this state the system output is lower than its initial state before learning, while the slow learner is not. The advantage of this is that when the setpoint returns to +1, the overall learning process is faster than the initial learning (compare the rise in the blue curves on the first and second occurrences of the setpoint +1). This is because the slow learner has retained much of the learning, thereby demonstrating savings and spontaneous recovery of previously learned memories [27].

Although the original DL shows a fast learning process, it still has a steady-state error. To overcome this problem, we introduce an additional integrator component in the two learners, resulting in our DIL. Thus, the DIL becomes a two-state gain-integral multi-rate model defined by the following simple equations:

$$
\begin{aligned}
x_f(n) &= A_f \cdot x_f(n-1) + B_f \cdot e(n) + C_f \cdot \int e(n) \\
x_s(n) &= A_s \cdot x_s(n-1) + B_s \cdot e(n) + C_s \cdot \int e(n) \\
x(n) &= x_s(n) + x_f(n) \\
e(n) &= f(n) - x(n)
\end{aligned}
\tag{2}
$$

where $x_f(n)$ and $x_s(n)$ are the states of the fast and slow learners, respectively, each consisting of three terms. The computation of each learner state is simple. The first term is a multiplication of the previous learner state ($x_{f,s}(n-1)$) and the constant retention factor ($A_{f,s}$). The second term is a multiplication of the current error feedback ($e(n)$) and the constant learning rate ($B_{f,s}$). The final term is a multiplication of the integrated or summed error ($\int e(n)$) over time and the constant integral rate ($C_{f,s}$). This term basically forces the learning process to correct the error. It should be noted that the new parameters are under the constraints of $C_f > C_s$. Thus, the fast learner learns the accumulated error more rapidly. A simulation of the learning process in the DIL is shown in Fig. 3. This illustrates that it retains the advantages of the original DL while also removing the steady-state error.

To use the DIL to adapt the frequency of a CPG controlling a legged robotic system, we use the neural SO(2)-oscillator based CPG model [8] together with the DIL-SO(2) network shown in Fig. 4a. This CPG model consists of two fully connected additive time-discrete neurons, both using the sigmoidal transfer function (see (III) in Fig. 4a). The synaptic weight matrix is chosen according to the following:

$$
\begin{pmatrix} W_{00}(t) & W_{01}(t) \\ W_{10}(t) & W_{11}(t) \end{pmatrix} = \alpha \cdot \begin{pmatrix} \cos\varphi(t) & \sin\varphi(t) \\ -\sin\varphi(t) & \cos\varphi(t) \end{pmatrix}
\tag{3}
$$

where W_{00-11} are synaptic weights in the CPG, α is a constant that determines the amplitude and the nonlinearity of the CPG, and φ is a frequency determining parameter. The outputs of the SO(2) oscillator are given as position commands to the joints of the legged robotic system (see (V) in Fig. 4a and black arrows in 4b). The DIL (see (II) in Fig. 4a) adapts
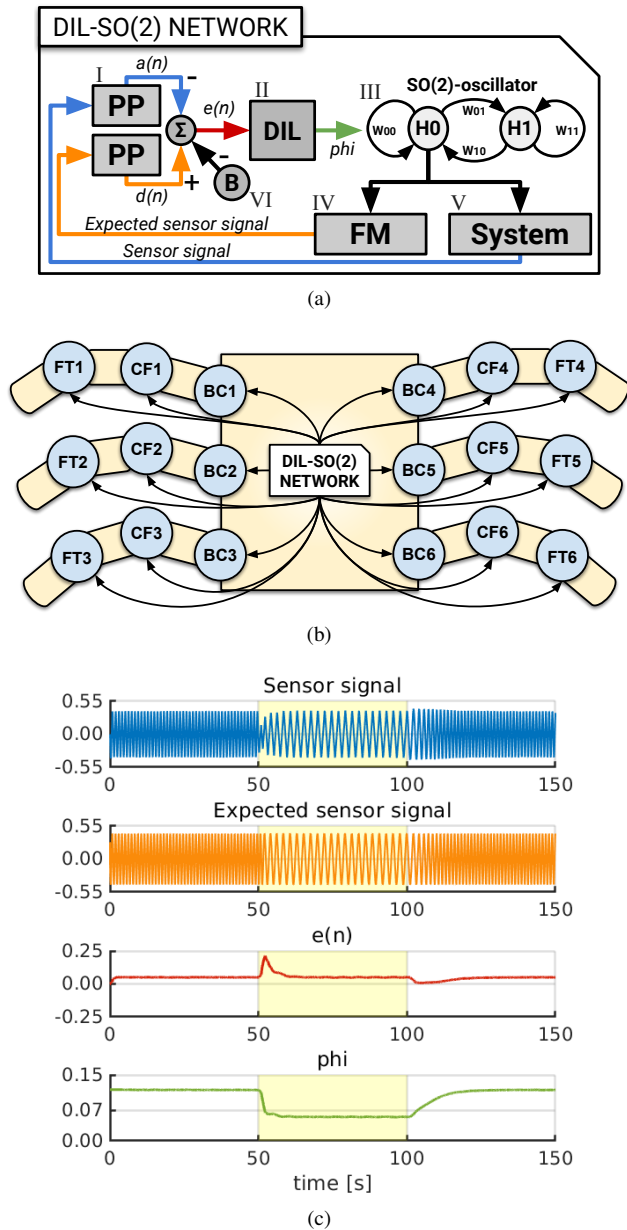
(a)

(b)

(c)

Fig. 4. **(a)** The DIL-SO(2) network that combines the DIL and the neural SO(2)-oscillator based CPG model for robot locomotion control. The CPG model is used to generate a rhythmic signal while the DIL is used to reduce the tracking error by adapting the CPG frequency. **(b)** The DIL-SO(2) network when used to control the joints of a hexapod robot. **(c)** Simulation of the network when used to reduce tracking errors. The maximum frequency of the system is reduced in the yellow zone from 50s to 100s.

φ (i.e., $\varphi = x(n)$) based on the error feedback (red arrow, $e(n)$) given as the tracking error between the amplitude of the actual joint angle sensory signals (blue arrows, $a(n)$) and the desired rhythmic joint movements (orange arrows, $d(n)$) as generated by the CPG signal (i.e., $e(n) = d(n) - a(n)$). The amplitudes of the signals are calculated using post-processing units (see (I) in Fig. 4a) which also use a digital Low-Pass Single-Pole IIR filter to remove noise. To compare the CPG output with the joint angle sensors in the system, a forward model is used (see (IV) in Fig. 4a). The forward model is modelled as a simple gain and can translate the CPG output

into an expected sensor signal. If the amplitude of the expected sensor signal is larger than the amplitude of the actual sensor signal (i.e., positive tracking error), then the DIL decreases the CPG frequency (i.e., φ) as the joint does not have enough time to follow the given rhythmic trajectory. However, in the case of tracking error, it does not make sense to consider negative errors since it is fair to assume that the joint will not move more than what the CPG is telling them to. A problem thus occurs if the mechanism should also have the ability to increase the CPG frequency. To address this issue, a small bias (see (VI) in Fig. 4a) can be subtracted from the tracking error. The DIL mechanism will in this way sense a negative tracking error when the desired and actual amplitudes match and try to increase the CPG frequency. An example of the DIL for frequency adaptation is shown in Fig. 4c. The maximum frequency of the system reduces after 50s and increases again after 100s where it returns to the initial state. As can be observed at 50s and 100s the DIL quickly adapts the CPG frequency to fit the performance of the system. For the experiments presented in Sect. III, the joint angle sensory signal from a shoulder joint (see BC1 joint in Fig. 4b) in the legged robots (shown later) is used as the actual sensor signal. The reason for using this joint is that it is responsible for moving the robot forward during the stance phase and thus also directly specifies the walking speed.

When using feedback from a single joint the outputs of both the FM and system (see (IV) and (V) in Fig. 4a) have a dimension of one. However, the DIL-SO(2) network is scalable, meaning that it can take multiple joint sensory values and calculate an average tracking error. Therefore, depending on the application, it can be used for controlling a single joint or multiple joints which may be useful in decentralized controllers like the one shown in [28] where each leg has its own CPG.

B. Correlation-based Learning

To subsequently compare the performance of error-based learning for frequency adaptation we use the state-of-the-art correlation-based learning mechanism AFDC by Nachstedt et al. [17]. In contrast to traditional adaptive frequency oscillators (AFOs), AFDC provides both faster and more precise adaptation for a wide range of target frequencies without the need for parameter fine-tuning. It accomplishes this by dynamically adapting the coupling strength of an external perturbation signal to a CPG. This makes it very attractive for locomotion controllers which need to react fast to external perturbations and the environment.

Nachstedt et al. [17] showed how to equip the Hopf, Van der Pol [6], and neural SO(2) [8] oscillators with the AFDC mechanism. In the following section, we only show the method for implementing it on the neural SO(2)-oscillator since we use this model to validate our mechanism.

To establish dynamic coupling, a single extra neuron (H_2) is connected to the SO(2)-oscillator through plastic synapses, W_{20} and W_{02} (dashed lines in Fig. 5). This extra neuron calculates a filtered version of the external signal, F, and receives signals via the synapses W_{20} and W_{2F} governed by the following rules:
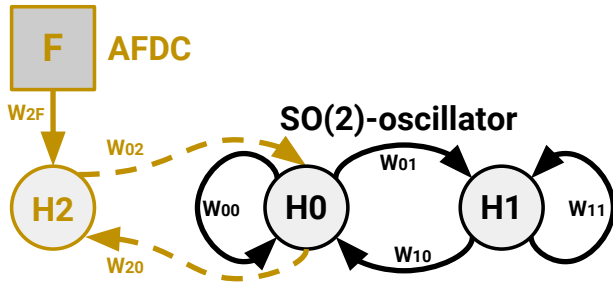
Fig. 5. Implementation of the AFDC on the SO(2)-oscillator. The light brown parts represent the AFDC mechanism, consisting of a single neuron (H_2)), enabling the oscillator to synchronize its frequency with the external perturbation or movement-related sensory feedback F. The black parts represent the SO(2)-oscillator, consisting of two fully connected neurons (H_0 and H_1).
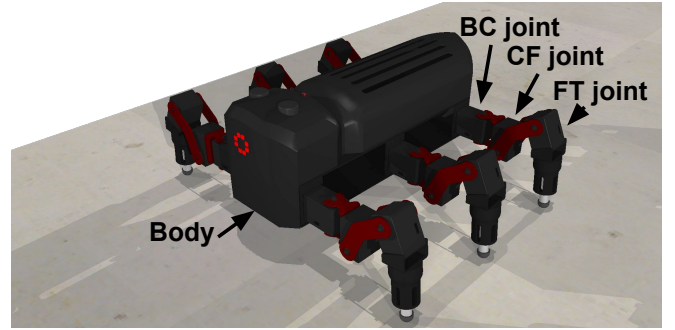

Fig. 6. Simulation of the MORF robot developed by Thor et al. [35]. Each leg consists of three segments (coxa, femur, and tibia) and three joints (BC (body-coxa), CF (coxa-femur), and FT (femur-tibia)).

$$W_{20}(t + 1) = W_{20}(t) + (\beta_0 - W_{20}(t) - \kappa \cdot o_2(t) \cdot o_0(t))/\tau$$
$$W_{2F}(t + 1) = W_{2F}(t) + (\epsilon_0 - W_{2F}(t) - \kappa \cdot F(t) \cdot o_2(t))/\tau$$
$$(4)$$

where β and ϵ are adaptive coupling strengths, κ is the correlation learning rate, τ is a time constant, o_0 is the output from neuron H_0, and o_2 is the output from neuron H_2. The output from H_2 can be seen as the weighted difference between the external signal F (i.e., sensory feedback) and the activity value of H_0. If the difference between the intrinsic frequency and target frequency of F is high, the coupling strength is increased to accelerate the adaptation. On the other hand, if the difference is small, then the coupling strength is reduced to increase the precision of the adaptation.

Finally, the frequency determining value φ of the oscillator is modulated by the AFDC using the following adaptation rule:

$$\varphi(t + 1) = \varphi(t) + \eta \cdot W_{02}(t) \cdot o_2(t) \cdot W_{01}(t + 1) \cdot o_1(t) \quad (5)$$

where o_1 is the output from H_1 and η is the learning rate. In this way, the synaptic plasticity converges when a certain or desired phase shift is achieved between the output of neuron H_0 and the external signal.

In [29] Nachstedt et al. described a method for using the AFDC to adapt the frequency of a CPG controlling the six-legged robot AMOS II [9]. The goal was to achieve more energy-efficient locomotion and adapt the frequency in the case of inclination. For external perturbation to the AFDC, the joint angle sensory signal from a shoulder joint (i.e., BC joint) was used for the same reasons stated in Sect. II-A. Once again, it should be noted that the frequency of the CPG converges when the phase shift between the output neuron H_0 and the external perturbation signal reaches the desired or given point. However, for complex systems, such as legged robots, it is not clear which phase shift, $\Delta\phi$, between a motor command and a joint angle sensory signal will be optimal. Nachstedt et al. [29] tested various values for $\Delta\phi$. For flat terrain, it was found that a phase shift of $\Delta\phi = 0.2\pi$ produced the fastest and most energy-efficient locomotion, but also that further increase did not have any significant influence. In the following explained experimental setups, a phase shift of 0.2π between the CPG signal and the BC joint angle sensory signal is therefore used when testing the AFDC.
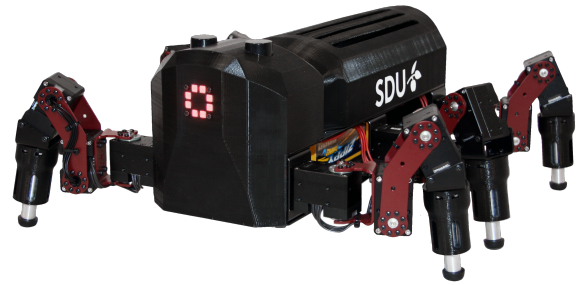
Fig. 7. Real-world version of the MORF robot developed by Thor et al. [35].

III. EXPERIMENTS

It should now be clear that the correlation-based learning mechanism (AFDC) adapts the phase shift between the CPG signal and joint angle sensory signal, while the error-based learning mechanism (DIL) reduces the tracking error between the two signals. To compare the performance of the two mechanisms, three legged-robot platforms have been simulated. A legged robot needs legs with at least two degrees of freedom to move - one for lifting and one for swinging - but is commonly equipped with legs that have three to allow for additional maneuvering [30]. Many of today's approaches to robot locomotion rely on CPG-based controllers [1], [31], [32], [33], as most locomotion behaviors are based on rhythmic and smooth motion (e.g., walking, swimming, flying, etc. [34]). This makes legged robots ideal for testing CPG learning mechanisms.

The first simulated platform (Fig. 6) is based on the real world hexapod robot called MORF developed by Thor et al. [35] as shown in Fig. 7. Each leg of MORF consists of three leg segments (coxa, femur, tibia) and three joints: the BC (body-coxa), CF (coxa-femur), and FT (femur-tibia) joints. This platform is used to verify that the proposed mechanism will work in a realistic setup. The second and third simulated platforms (Figs. 8 and 9) are only equipped with one leg consisting of the same leg segments and joints as MORF. A single leg is sufficient for testing the performance of our learning mechanism but insufficient to generate stable locomotion. The bodies of the second and third platform are thus placed on low friction sleds to ensure the robots are kept stable and upright during walking. It is expected that this approximation
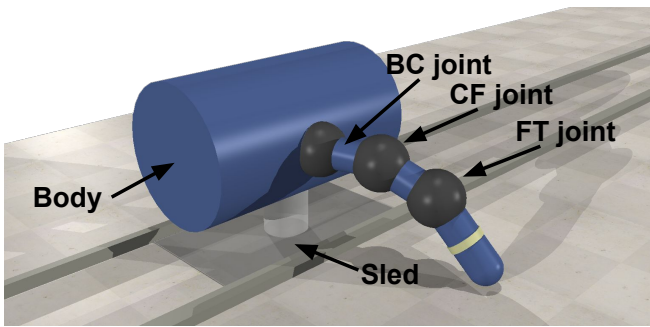
Fig. 8. Single-legged robot with a short leg and light body placed on a low friction sled. The leg consists of three segments (coxa, femur, and tibia) and three joints (BC (body-coxa), CF (coxa-femur), and FT (femur-tibia)).
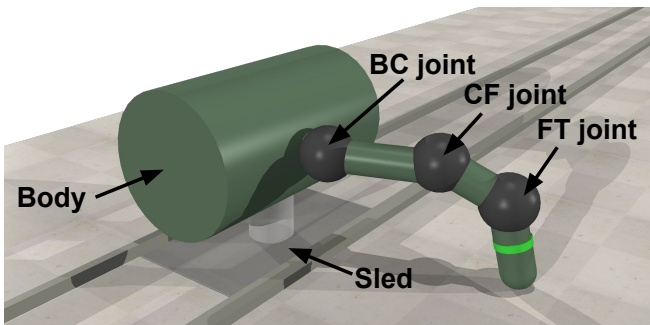

Fig. 9. Single-legged robot with a long leg and heavy body placed on a low friction sled. The leg consists of three segments (coxa, femur, and tibia) and three joints (BC (body-coxa), CF (coxa-femur), and FT (femur-tibia)).

will consume less energy as only one leg is used to move the body. However, since both mechanisms (AFDC and DIL) are tested on the same robot, it is still possible to compare their relative performance. The two single-legged platforms are also used to show generality and adaptability of the mechanisms. Consequently, they vary in morphology, weight, and range of motion which are typical variations between different kinds of legged robots. The first single-legged robot (Fig. 8) is light (1.00 kg) with a short leg (0.25 m) and a small range of motion for the BC joint (0.45 rad), while the second single-legged robot (Fig. 9) is heavier (2.50 kg) with a longer leg (0.33 m) and a larger range of motion for the BC joint (0.5 rad). The robot with the long leg, extra weight, and larger range of motion requires extra joint strain when compared to the one with a short leg, and therefore, the frequency mechanisms need to adapt accordingly.

The three robots are all simulated using the versatile, scalable, and powerful general-purpose robot simulation framework called V-REP [36]. The simulated environment offers real-world parameters (i.e., corresponding to physical units) for a large number of physical properties, making it both realistic and precise. To test the robustness of the mechanisms, Gaussian noise with a variance of $5.0 \cdot 10^{-2}$ radians is introduced to the joint angle sensors of the robotic systems. The actual noise distribution for joint angle sensors in legged robots is unknown and depends heavily on the underlying robot system, especially in relation to the kinematics, the tolerances, the way the joints are controlled, as well as the joint

sensors themselves. However, it is fair to say that the amount of noise introduced is higher than typically expected from joint angle sensors and therefore, serves as a worst-case scenario. This is because the noise often boils down to the resolution of the analog to digital converter (ADC) and encoder if the digital signal remains clean.

All three platforms are controlled using the neural SO(2)-oscillator based CPG under the assumption that the periodic shape of the CPG is given, and only frequency optimization is required. The simulated MORF robot uses a fixed phase relationship between its six legs, giving it a static tripod gait, resulting in static stability. This is because the center of mass of the robot will always be within the support polygon (defined as the convex polygon formed by connecting the three footprints). As described earlier, error feedback to the DIL is defined as the tracking error between the amplitude of one BC joint angle sensory signal and the amplitude of the CPG output that drives it (efference copy). The BC joint angle sensory signal is likewise used as the external perturbation to the AFDC mechanism.

Each platform is tested ten times using no frequency adaptation (NA), the original DL, AFDC, and DIL. NA is expected to be the worst and functions as a control mechanism for the hypothesis that adapting the CPG frequency results in lower error and more energy-efficient locomotion. The DL is expected to perform worse than the DIL since it will not be able to remove the steady-state error (see Fig. 2). During walking, the stimulus changes twice; after the motor power is reduced at 200s and after it recovers at 400s. The initial frequency for each experiment is set on the basis of the converted frequency from the AFDC mechanism since that is currently state-of-the-art. In this way, the AFDC, DL, and DIL adaptation mechanisms will have a fair starting point. All joints in the three platforms are modeled as MX-106 smart servos from Dynamixel, and the reduction in motor power is equivalent to lowering the power to each motor by 1.5 amperes. It should be noted that the same CPG drives all joints in each platform and all joints also experience the same reduction in motor power since they are assumed to be connected to the same power source.

The three platforms are equipped with identical learning parameters for the DL and DIL mechanism; $A_f = 0.2$, $A_s = 0.4$, $B_f = 0.2$, $B_s = 2.0 \cdot 10^{-2}$, $C_f = 8.0 \cdot 10^{-3}$, and $C_s = 8.0 \cdot 10^{-4}$, whereas DL only uses A_f, A_s, B_f, and B_s. This is to show that the parameters are not sensitive to different robot systems. In other words, we do not need to precisely adjust the parameters for specific robots. For all three platforms, the same bias of $5.0 \cdot 10^{-2}$ is used which allowed the DL and DIL mechanisms to increase the CPG frequency while maintaining a low tracking error. The parameters for the AFDC in all three platforms are set as specified in [29] for the experiments with AMOS II and the phase shift between the CPG signal and BC joint angle sensory signal is set to $\Delta\phi = 0.2\pi$.

The following data is logged for each platform using one of the adaptation mechanisms: the frequency determining variable φ, mean tracking error, and mean cost of transport (COT) calculated as $\frac{P}{m \cdot g \cdot v}$, where m is the weight of the entire robot in kg, g is the gravity of earth ($9.82 m/s^2$), v is the walking
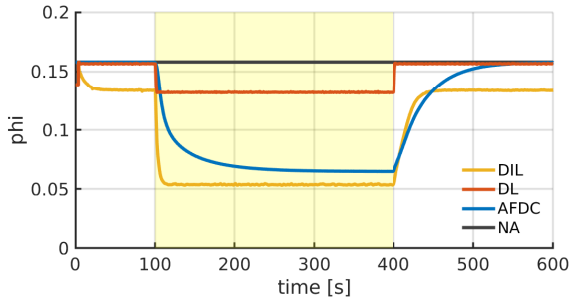
Fig. 10. Adaptation of the CPG frequency determining parameter φ using the three mechanisms on the MORF hexapod robot. The yellow zone indicates a reduction in the motor power.
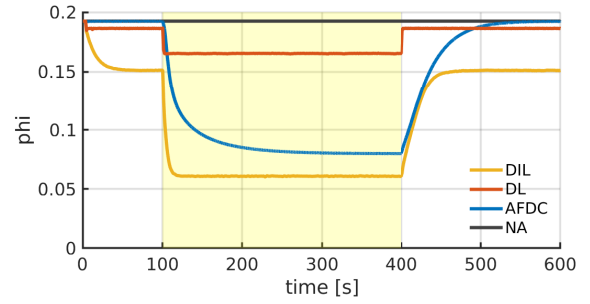

Fig. 13. Adaptation of the CPG frequency determining parameter φ using the three mechanisms on the robot with a light body and short leg. The yellow zone indicates a reduction in the motor power.
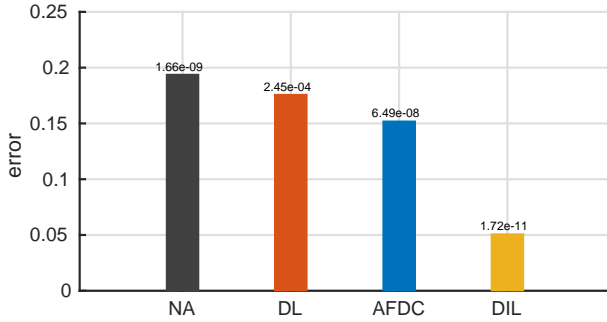

Fig. 11. Mean tracking error between the CPG output and BC joint angle signal of the three mechanisms when used on the MORF hexapod robot.
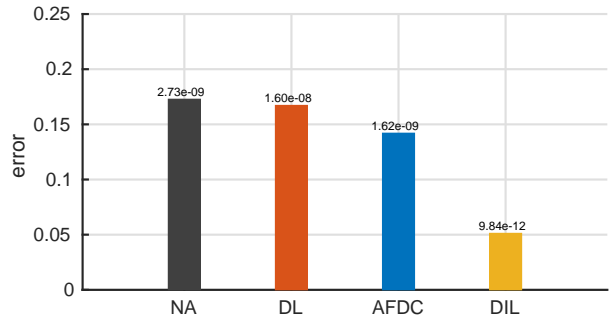

Fig. 14. Mean tracking error between the CPG output and BC joint angle signal of the three mechanisms when used on the robot with a light body and short leg.
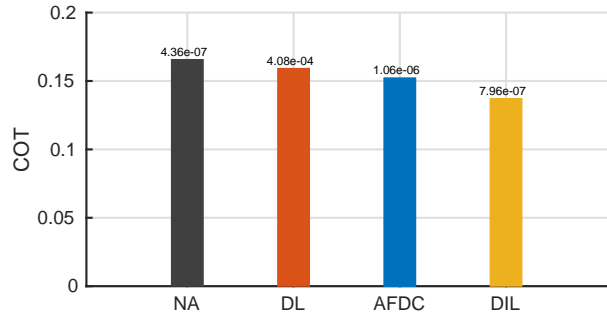

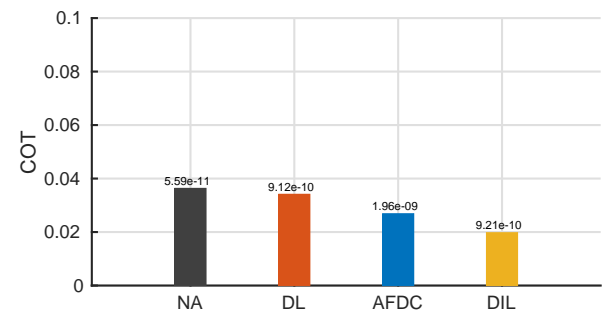Fig. 12. Mean cost of transport for the three mechanisms when used on the MORF hexapod robot.

Fig. 15. Mean cost of transport for the three mechanisms when used on the robot with a light body and short leg.

velocity of the robot in m/s, and P is the power given as the joint torque in $N \cdot m$ times the angular joint velocity in rad/s. It should be noted that COT is a dimensionless measurement that quantifies the energy efficiency of transporting the legged robot from start to finish positions (i.e., the energy efficiency of the generated locomotion).

IV. RESULTS

A. Testing the MORF hexapod robot

In this section, we present the results of the experiments with the simulated MORF hexapod robot (shown in Fig. 6). The plot in Fig. 10 shows the CPG frequencies of the four mechanisms. The power to the motors is set to reduce by 1.5 amperes from 200s and 400s (yellow zone). The bar plot in Fig. 11 shows the mean tracking error between the BC joint

angle sensor signal of a middle leg and the desired movement generated by the CPG. The bar plot in Fig. 12 shows the mean COT for the robot. It should be noted that the variance is specified above each bar in both bar plots.

By definition, the frequency using NA is constant, resulting in a high error and COT. On the other hand, the DL is able to adapt the CPG frequency when the motor power is reduced and after recovery. This results in a lower tracking error ($P >$ .999) and COT ($P >$ .999) in comparison to the NA. The AFDC mechanism is likewise able to adapt the CPG frequency and is better at reducing the tracking error ($P >$ .999) and COT ($P >$ .999) in comparison to the DL. Finally, the DIL mechanism can reduce the tracking error ($P >$ .999) and COT ($P >$ .999) even further in comparison to the AFDC. It should be noted that all three mechanisms have low variances, thereby showing robustness to the added noise. This is also the reason

for very convincing P-values.

B. Testing the robot with a light body and short leg

Here we present the results of the experiments for the single-legged robot with a light body and short leg (shown in Fig. 8). Figs. 13, 14, and 15 display the same information as explained in the previous section.

When comparing the DL with NA, it is clear that the DL has a lower COT ($P > .999$) and tracking error ($P > .999$). Again, AFDC is better at reducing the COT ($P > .999$) and tracking error ($P > .999$) compared to the DL. Finally, in this case, the DIL is also able to reduce the COT ($P > .999$) and tracking error ($P > .999$) even further than the AFDC. Once again, it should be noted that all three mechanisms have low variances; thereby showing robustness against the added noise.

C. Testing the robot with a heavy body and long leg

Finally, we present the results of the experiments with the robot with a heavy body and single long leg (shown in Fig. 9). Figs. 16, 17, and 18 display the same information as explained in Sec. IV-A.

When comparing the DL with NA, again, it is clear that the DL has a lower COT ($P > .999$) and tracking error ($P > .999$). In this case, the AFDC is also able to reduce the COT ($P > .999$) and tracking error ($P > .999$) when compared to the DL. Finally, once again, the DIL is able to reduce the COT ($P > .999$) and tracking error ($P > .999$) even further when compared to the AFDC. It should be noted that all three mechanisms also have low variances on this test platform.

V. DISCUSSION

In this paper, we introduce the use of an error-based learning mechanism for quickly adapting the frequency of a CPG. The results show that our error-based mechanism (DIL) reduces the tracking error by adapting the CPG frequency to enable the system to follow the generated trajectory. When compared to a state-of-the-art correlation-based mechanism (AFDC), it is clear that the error-based mechanism is faster at adapting, better at reducing the tracking and steady-state error, and can generate more energy-efficient locomotion (i.e., COT). Another drawback of the AFDC is that it changes the amplitude of the CPG signal during adaptation as a consequence of increasing the amplitude of the external perturbation signal during fast adaptation (see [17]). This increases the range of motion for the legs of the robot and in the worst case causes them to collide. This is not the case for the DIL which only regulates the frequency by determining the synaptic weights of the SO(2)-oscillator.

The results also show that the DL is not able to reduce the tracking error as much as the DIL (Sect. II-A). Reducing the tracking error results in more energy-efficient locomotion, as indicated by the positive linear correlation between tracking error and COT for all three platforms. This is presumably because leg movement with low tracking error has longer stance phase and does not have to change direction as often. Furthermore, a leg with low tracking error follows the
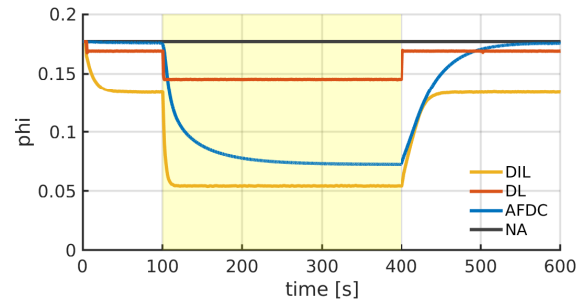

Fig. 16. Adaptation of the CPG frequency determining parameter φ using the three mechanisms on the robot with a heavy body and long leg. The yellow zone indicates a reduction in the motor power.
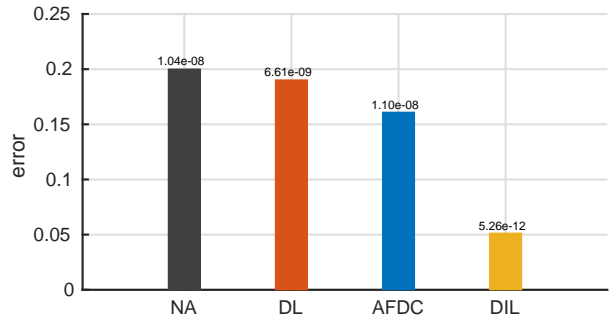

Fig. 17. Mean tracking error between the CPG output and BC joint angle signal of the three mechanisms when used on the robot with a heavy body and long leg.
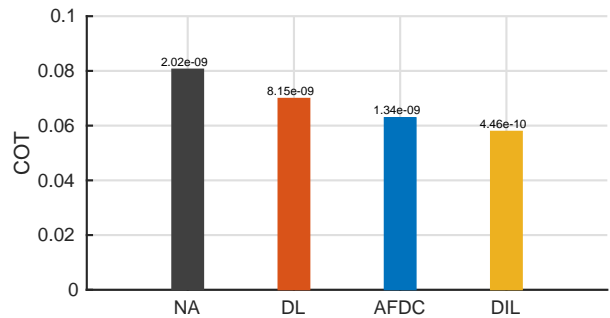

Fig. 18. Mean cost of transport for the three mechanisms when used on the robot with a heavy body and long leg.

generated trajectory better, which in the case of this study is arbitrarily chosen. It is, however, fair to assume that the trajectories emerging from the fact that the leg cannot follow the original trajectory (due to the rapid change of direction, short stance phases, asymmetric BC rotations, etc.) are less energy-efficient.

The AFDC and other correlation-based learning mechanisms, [14], [16], reduce tracking error by tuning the frequency toward the desired phase shift, and often the systems resonant frequency. However, for complex systems, such a frequency is not always possible to derive, and the phase shift, therefore, has to be empirically chosen. Furthermore, in the case of legged robots, a phase shift that guarantees near optimal locomotion is hard to find [29] since there is no intuitive correlation between phase shift and tracking error. This is not the case for error-based learning mechanisms since they can reduce

energy usage during locomotion by reducing the tracking error. This is an advantage for studies where the entire trajectory is expected to be utilized by the system. Since the control parameters of the DIL and many other error-based learning mechanisms can easily relate to the error reduction, i.e., gain and integrator terms, the DIL is also easier to tune in complex systems. When compared to other learning mechanisms, such as fuzzy-based multi-error constraint control [37] and neural network-based model-free adaptive fault-tolerant control [38], the DIL does not require any neural networks, compact form dynamic linearization data models, fuzzy logic systems, or system knowledge. The DIL, therefore, has less computational complexity and is easily integrated into a complex robotic system.

Finally, the results show that both the AFDC and DIL are robust against the added sensor noise as indicated by their small variance in both error and COT. The reason for the robustness of the DIL mechanism stems from the fact that the signals are low-pass filtered prior to calculation of the amplitudes. If the low-pass filters are unable to remove big spikes of noise, the pre-processor unit potentially calculates faulty amplitudes which are considerably smaller than the real ones, resulting in sudden and significant frequency adjustment. This effect is not desired, so the low-pass filters should be tuned accordingly to the expected noise level.

For future study, we plan to validate the DIL using a real-world version of the six-legged robot MORF as shown in Fig. 7 and on other types of robotic systems such as a robotic arm. Further investigation is also proposed into the correlation between energy-efficient locomotion and tracking error since it seems as though correlation-based learning mechanisms are also converging toward frequencies of near-zero tracking error [14], [17]. Finally, we plan to investigate whether or not the control parameters of the DIL or other error-based learning mechanisms can be related to the frequency of the CPG. In this way, it might be possible to tune the learning mechanisms in a principled way, rather than experimentally determining the parameters.

VI. CONCLUSION

This paper demonstrates that our novel error-based learning mechanism called the DIL can be used to quickly reduce the tracking error when applied to legged robots. It does this by adapting the CPG frequency to enable the system to follow the trajectory as generated by the CPG. In other words, the mechanism ensures that the CPG frequency matches the performance of the robotic system. When compared to the state-of-the-art correlation-based learning mechanism called AFDC, the error-based learning mechanism is both faster at adapting and better at reducing tracking and steady-state errors, resulting in more energy-efficient locomotion. Furthermore, the DIL is insensitive to control parameter settings for specific robots where all robot experiments use the same parameters ($A_{s,f}$, $B_{s,f}$, $C_{s,f}$).

The fact that DIL matches the CPG frequency with the performance of the robotic system and that the entire generated trajectory is followed with low tracking and steady-state errors

may significantly improve research concerning trajectory optimization, universal controllers, and other studies in relation to the change of intrinsic or extrinsic parameters. For future study on energy-efficient locomotion, our findings indicate that it might be advantageous to focus on adapting the CPG frequency by minimizing tracking error.

REFERENCES

[1] A. J. Ijspeert, "Central pattern generators for locomotion control in animals and robots: A review," *Neural Networks*, vol. 21, no. 4, pp. 642 – 653, 2008.

[2] J. Yu, M. Tan, J. Chen, and J. Zhang, "A survey on CPG-inspired control models and system implementation," *IEEE Transactions on Neural Networks and Learning Systems*, vol. 25, no. 3, pp. 441–456, March 2014.

[3] T. G. Brown, "On the nature of the fundamental activity of the nervous centres; together with an analysis of the conditioning of rhythmic activity in progression, and a theory of the evolution of function in the nervous system," *The Journal of Physiology*, vol. 48, no. 1, pp. 18–46, 1914.

[4] J. Hellgren, S. Grillner, and A. Lansner, "Computer simulation of the segmental neural network generating locomotion in lamprey by using populations of network interneurons," *Biological Cybernetics*, vol. 68, no. 1, pp. 1–13, Nov 1992.

[5] Ö. Ekeberg, "A combined neuronal and mechanical model of fish swimming," *Biological Cybernetics*, vol. 69, no. 5, pp. 363–374, Oct 1993.

[6] B. van der Pol, "On relaxation-oscillations," *The London, Edinburgh, and Dublin Philosophical Magazine and Journal of Science*, vol. 2, no. 11, pp. 978–992, 1926.

[7] K. Matsuoka, "Sustained oscillations generated by mutually inhibiting neurons with adaptation," *Biological Cybernetics*, vol. 52, no. 6, pp. 367–376, Oct 1985.

[8] F. Pasemann, M. Hild, and K. Zahedi, "So(2)-networks as neural oscillators," in *Proc. of Computational Methods in Neural Modeling*, J. Mira and J. R. Álvarez, Eds. Berlin, Heidelberg: Springer Berlin Heidelberg, 2003, pp. 144–151.

[9] P. Manoonpong, U. Parlitz, and F. Wörgötter, "Neural control and adaptive neural forward models for insect-like, energy-efficient, and adaptable locomotion of walking machines," *Frontiers in Neural Circuits*, vol. 7, p. 12, 2013.

[10] M. Jouaiti, L. Caron, and P. Hnaff, "Hebbian plasticity in CPG controllers facilitates self-synchronization for human-robot handshaking," *Frontiers in Neurorobotics*, vol. 12, p. 29, 2018.

[11] D. Owaki, T. Kano, K. Nagasawa, A. Tero, and A. Ishiguro, "Simple robot suggests physical interlimb communication is essential for quadruped walking," *Journal of The Royal Society Interface*, vol. 10, no. 78, 2013.

[12] T. Sun, D. Shao, Z. Dai, and P. Manoonpong, "Adaptive neural control for self-organized locomotion and obstacle negotiation of quadruped robots," in *Proc. of 27th IEEE International Conference on Robot and Human Interactive Communication*, 2018, pp. 1081–1086.

[13] P. Arena, A. Bonanzinga, and L. Patané, "Role of feedback and local coupling in CNNs for locomotion control of a quadruped robot," in *Proc. CNNA 2018; The 16th International Workshop on Cellular Nanoscale Networks and their Applications*, Aug 2018, pp. 1–4.

[14] M. Khoramshahi, R. Nasiri, M. Shushtari, A. J. Ijspeert, and M. N. Ahmadabadi, "Adaptive natural oscillator to exploit natural dynamics for energy efficiency," *Robotics and Autonomous Systems*, vol. 97, pp. 51 – 60, 2017.

[15] G. Taga, Y. Yamaguchi, and H. Shimizu, "Self-organized control of bipedal locomotion by neural oscillators in unpredictable environment," *Biological Cybernetics*, vol. 65, no. 3, pp. 147–159, Jul 1991.

[16] L. Righetti, J. Buchli, and A. J. Ijspeert, "Dynamic Hebbian learning in adaptive frequency oscillators," *Physica D: Nonlinear Phenomena*, vol. 216, no. 2, pp. 269 – 281, 2006.

[17] T. Nachstedt, C. Tetzlaff, and P. Manoonpong, "Fast dynamical coupling enhances frequency adaptation of oscillators for robotic locomotion control," *Frontiers in Neurorobotics*, vol. 11, p. 14, 2017.

[18] K. Furuta, "Control of pendulum: from super mechano-system to human adaptive mechatronics," in *42nd IEEE International Conference on Decision and Control (IEEE Cat. No.03CH37475)*, vol. 2, Dec 2003, pp. 1498–1507 Vol.2.

[19] T. Nachstedt, F. Wörgötter, and P. Manoonpong, "Adaptive neural oscillator with synaptic plasticity enabling fast resonance tuning," in *Artificial Neural Networks and Machine Learning – ICANN 2012*, A. E. P. Villa, W. Duch, P. Érdi, F. Masulli, and G. Palm, Eds. Berlin, Heidelberg: Springer Berlin Heidelberg, 2012, pp. 451–458.

[20] T. Wang, Y. Hu, and J. Liang, "Learning to swim: a dynamical systems approach to mimicking fish swimming with CPG," *Robotica*, vol. 31, no. 3, p. 361369, 2013.

[21] L. Righetti, J. Buchli, and A. J. Ijspeert, "Adaptive Frequency Oscillators and Applications," *The Open Cybernetics & Systemics Journal*, vol. 3, no. 2, pp. 64–69, 2009.

[22] R. Ronsse, J. Kieboom, and A. Ijspeert, "Automatic resonance tuning and feedforward learning of biped walking using adaptive oscillators," in *Proc. of Multibody Dynamics 2011, ECCOMAS Thematic Conference*, 2011, pp. 4–7.

[23] C. P. Santos, N. Alves, and J. C. Moreno, "Biped locomotion control through a biomimetic CPG-based controller," *Journal of Intelligent & Robotic Systems*, vol. 85, no. 1, pp. 47–70, Jan 2017.

[24] T. Nachstedt, F. Wrgtter, P. Manoonpong, R. Ariizumi, Y. Ambe, and F. Matsuno, "Adaptive neural oscillators with synaptic plasticity for locomotion control of a snake-like robot with screw-drive mechanism," in *2013 IEEE International Conference on Robotics and Automation*, May 2013, pp. 3389–3395.

[25] M. A. Smith, A. Ghazizadeh, and R. Shadmehr, "Interacting adaptive processes with different timescales underlie short-term motor learning," *PLOS Biology*, vol. 4, no. 6, pp. 1035–1043, 5 2006.

[26] Y. Kojima, Y. Iwamoto, and K. Yoshida, "Memory of learning facilitates saccadic adaptation in the monkey." *The Journal of neuroscience : the official journal of the Society for Neuroscience*, vol. 24, pp. 7531–7539, 2004.

[27] D. M. Wolpert, J. Diedrichsen, and J. R. Flanagan, "Principles of sensorimotor learning," *Nature Reviews Neuroscience*, vol. 12, pp. 739–751, oct 2011.

[28] S. S. Barikhan, F. Wörgötter, and P. Manoonpong, "Multiple decoupled CPGs with local sensory feedback for adaptive locomotion behaviors of bio-inspired walking robots," in *From Animals to Animats 13*, A. P. del Pobil, E. Chinellato, E. Martinez-Martin, J. Hallam, E. Cervera, and A. Morales, Eds. Cham: Springer International Publishing, 2014, pp. 65–75.

[29] T. Nachstedt, "Adaptive neural oscillator with synaptic plasticity for robot locomotion control," Master's thesis, Georg-August-Universität Göttingen, Wilhelmsplatz 1 (Aula) 37073 Göttingen, 3 2013.

[30] R. Siegwart and I. R. Nourbakhsh, *Introduction to Autonomous Mobile Robots*, ser. Intelligent robotics and autonomous agents. MIT, 2004.

[31] H. Yu, W. Guo, J. Deng, M. Li, and H. Cai, "A CPG-based locomotion control architecture for hexapod robot," in *Proc. of 2013 IEEE/RSJ International Conference on Intelligent Robots and Systems*, Nov 2013, pp. 5615–5621.

[32] K. Aparna, S. Geeta, K. Kirtee, and J. Madhuri, "CPGs Inspired Adaptive Locomotion Control for Hexapod Robot," *International Journal of Engineering Science Invention*, vol. 2, no. 4, pp. 13–18, 2013.

[33] L. Minati, M. Frasca, N. Yoshimura, and Y. Koike, "Versatile Locomotion Control of a Hexapod Robot Using a Hierarchical Network of Nonlinear Oscillator Circuits," *IEEE Access*, vol. 6, pp. 8042–8065, 2018.

[34] T. Fukuda, Y. Hasegawa, K. Sekiyama, and T. Aoyama, *Multi-Locomotion Robotic Systems*, ser. Springer Tracts in Advanced Robotics. Springer-Verlag Berlin Heidelberg, 2012.

[35] M. Thor, J. C. Larsen, and P. Manoonpong, "MORF - Modular Robot Framework," in *Proc. of The 2nd International Youth Conference of Bionic Engineering (IYCBE2018)*. Frontiers, Nov. 2018, pp. 21–23.

[36] M. F. E. Rohmer, S. P. N. Singh, "V-rep: a versatile and scalable robot simulation framework," in *Proc. of The International Conference on Intelligent Robots and Systems (IROS)*, 2013.

[37] L. Liu, Y. Liu, and S. Tong, "Fuzzy based multi-error constraint control for switched nonlinear systems and its applications," *IEEE Transactions on Fuzzy Systems*, pp. 1–1, 2018.

[38] Z. Wang, L. Liu, and H. Zhang, "Neural Network-Based Model-Free Adaptive Fault-Tolerant Control for Discrete-Time Nonlinear Systems with Sensor Fault," *IEEE Transactions on Systems, Man, and Cybernetics: Systems*, vol. 47, no. 8, pp. 2351–2362, 2017.

Mathias Thor received an M.Sc. degree in Robot Systems from the University of Southern Denmark, Odense, Denmark, in 2019. He is currently pursuing a Ph.D. degree with SDU Embodied Systems for Robotics and Learning at the University of Southern Denmark. His current research interests include neural locomotion control of walking machines, learning/plasticity, dynamic simulations, and design of legged robotic systems including their software interface.

Poramate Manoonpong received a Ph.D. degree in Electrical Engineering and Computer Science from the University of Siegen, Siegen, Germany, in 2006. He was the Emmy Noether Research Group Leader for Neural Control, Memory, and Learning for Complex Behaviors in Multisensory-Motor Robotic Systems with the Bernstein Center for Computational Neuroscience, Georg-August Universität Göttingen, Göttingen, Germany, from 2011 to 2014. Currently, he is a professor at the College of Mechanical and Electrical Engineering at Nanjing University of Aeronautics and Astronautics (NUAA), China. He has been an invited Professor of School of Information Science & Technology at Vidyasirimedhi Institute of Science & Technology (VISTEC), Thailand, and has served as an Associate Professor of Embodied AI & Robotics at the University of Southern Denmark (SDU), Denmark. His current research interests include Embodied AI, machine learning for robotics, neural locomotion control of walking machines, biomechanics, dynamics of recurrent neural networks, learning/plasticity, embodied cognitive systems, prosthetic and orthopedic devices, exoskeletons, brain-machine interface, human-machine interaction, and service/inspection robots.